POLITECNICO DI TORINO
Repository ISTITUZIONALE

Analysis of the Steinmetz compensation circuit with distorted waveforms through symmetrical component-based indicators

(Article begins on next page)

19 May 2024

Analysis of the Steinmetz Compensation Circuit with Distorted Waveforms through Symmetrical Component-Based Indicators

Gianfranco Chicco, *Senior Member, IEEE*, Mircea Chindriş, *Member, IEEE*, Andrei Cziker, Petru Postolache, *Member, IEEE*, and Cornel Toader, *Member, IEEE*

Abstract – **This paper deals with the use of a set of indicators defined within a symmetrical component-based framework to study the characteristics of the Steinmetz compensation circuit in the presence of waveform distortion. The Steinmetz circuit is applied to obtain balanced currents in a three-phase system supplying a single-phase load. The circuit is analyzed without and with harmonic distortion of the supply voltages. The compensation effect is represented by the classical unbalance factor and by the Total Phase Unbalance (*TPU*) indicator defined in the symmetrical component-based framework. Comparing the two indicators, it is shown that the classical unbalance factor is insufficient to represent the effect of voltage distortion and fails to detect the lack of total unbalance compensation occurring with distorted waveforms. Correct information is provided by calculating the *TPU* indicator.**

Index Terms — **Steinmetz circuit, harmonics, symmetrical components, balanced currents, waveform distortion.**

I. INTRODUCTION

THE compensation of a three-phase circuit for obtaining balanced currents is one of the basic contributions of Steinmetz [1]. These concepts have been applied to various types of unbalanced systems and discussed in the light of adopting shunt compensation with static devices, since the beginning of these applications [2]. The Steinmetz circuitry represents a common solution to balance industrial high-power single-phase loads, without resorting to specific solutions with active filters. However, due to the use of supplementary reactive elements, the Steinmetz scheme has an asymmetric resonance behaviour in a range of relatively high frequencies and, thus, determines an asymmetric effect on the voltage harmonics. As a result, the system cannot be completely balanced when operating in harmonic distortion conditions. The interest towards the conceptual meaning and performance of the Steinmetz circuit has been revitalized in recent years [3], in the light of new theoretical advances based on the application of the Poynting vector [4], as well as for investigating harmonic response properties [5-9].

This paper addresses the Steinmetz compensation of unbalanced systems in the presence of distorted voltage and current waveforms. The symmetrical component framework developed in [10] and used in [11] is applied to show the benefits of using the extended indicators defined within this framework to combine the effects of unbalance and harmonic distortion. The specific features arising from the use of the extended indicators are compared to the classical unbalance factor ζ^u (i.e., the negative-to-positive sequence current ratio) and Total Harmonic Distortion (*THD*). With respect to various methods used in the literature for dealing with harmonics in unbalanced systems, for instance [12-15], the framework [10] provides explicit definitions of a set of balance, unbalance and distortion components, able to assist the characterization of the properties of the Steinmetz circuitry under waveform distortion by identifying to what extent the desired operation of such a circuitry is affected by the distortion components. The calculations are carried out on a simple scheme of unbalanced system taken from the recent literature [4], compensated by using the Steinmetz circuit with parameters set up according to the classical rules without considering waveform distortion. However, the nature of the results obtained is of general interest for any type of system to be compensated through the Steinmetz circuit.

II. EXTENDED PERFORMANCE INDICATORS FOR UNBALANCED THREE-PHASE SYSTEMS WITH DISTORTED WAVEFORMS

Starting from the three-phase current phasors at the harmonic order h ($\overline{I}_a^h$ at phase a, $\overline{I}_b^h$ at phase b and $\overline{I}_c^h$ at phase c), the transformed phase currents at the hth harmonic order, for $h = 1,\ldots, H$ (where for instance $H = 40$, as in the EN 50160 Standard [19]) are obtained through the symmetrical component transformation:

$$
\begin{vmatrix} \overline{I}_{T1}^h \\ \overline{I}_{T2}^h \\ \overline{I}_{T3}^h \end{vmatrix} = \frac{1}{3} \begin{vmatrix} 1 & e^{j\frac{2\pi}{3}} & e^{j\frac{4\pi}{3}} \\ 1 & e^{j\frac{4\pi}{3}} & e^{j\frac{2\pi}{3}} \\ 1 & 1 & 1 \end{vmatrix} \begin{vmatrix} \overline{I}_a^h \\ \overline{I}_b^h \\ \overline{I}_c^h \end{vmatrix}
\tag{1}
$$

where the subscripts 1 for *positive*-, 2 for *negative*-, 3 for *zero*–sequence) are preferred to the subscripts 1, 2, 0 for representing the three components of the current in the transformed space. Consistent notation is then set up for the definition of the extended indicators, formulated with reference to the transformed phase currents [10].

G. Chicco is with Politecnico di Torino, Dipartimento di Ingegneria Elettrica, corso Duca degli Abruzzi 24, 10129 Torino, Italy (e-mail gianfranco.chicco@polito.it).

M. Chindriş and A. Cziker are with Technical University of Cluj-Napoca, Str. C. Daicoviciu 15, 3400 Cluj-Napoca, Romania (e-mail: Mircea.Chindris@eps.utcluj.ro, Andrei.Cziker@eps.utcluj.ro).

P. Postolache and C. Toader are with Universitatea Politehnica din Bucureşti, Facultatea de Energetica, Splaiul Independenţei 313, Bucharest, Romania (e-mail petrupostolache@yahoo.com).

A. Formulation of the extended indicators

The extension of the *THD* to unbalanced systems is given by the Total Phase Distortion (*TPD*) indicator

$$TPD = \frac{\sqrt{\sum_{h=2}^{H}\left[\left(I_{T1}^{h}\right)^2 + \left(I_{T2}^{h}\right)^2 + \left(I_{T3}^{h}\right)^2\right]}}{\sqrt{\left(I_{T1}^{1}\right)^2 + \left(I_{T3}^{1}\right)^2 + \left(I_{T3}^{1}\right)^2}} \quad (2)$$

The extension of the unbalance indicator to systems with distorted currents is provided by the Total Phase Unbalance (*TPU*) indicator:

$$TPU = \frac{\sqrt{\sum_{n=0}^{\infty}\left[\left(I_{T2}^{3n+1}\right)^2 + \left(I_{T3}^{3n+1}\right)^2 + \left(I_{T1}^{3n+2}\right)^2 + \left(I_{T3}^{3n+2}\right)^2 + \left(I_{T1}^{3n+3}\right)^2 + \left(I_{T2}^{3n+3}\right)^2\right]}}{\sqrt{\sum_{n=0}^{\infty}\left[\left(I_{T1}^{3n+1}\right)^2 + \left(I_{T2}^{3n+2}\right)^2 + \left(I_{T3}^{3n+3}\right)^2\right]}} \quad (3)$$

More generally, the framework developed in [10] defines the balance, unbalance and distortion components of system currents and voltages, on the basis of which a number of related indicators are formulated. Furthermore, it provides an effective partitioning of the equivalent apparent power [20] into balance, unbalance and distortion components. The full notation adopts the superscripts *b* for balance, *u* for unbalance, *d* for distortion, 1 for the first harmonic, and the subscripts *p* for circuit phase, *I* for current and *E* for voltage.

Concerning the system currents, in [10] the *balance* phase current component is defined as

$$I_{p}^{b} = \sqrt{\sum_{n=0}^{\infty}\left[\left(I_{T1}^{3n+1}\right)^2 + \left(I_{T2}^{3n+2}\right)^2 + \left(I_{T3}^{3n+3}\right)^2\right]} \quad (4)$$

Considering only the entry of (4) at fundamental frequency, it is possible to define the balance *fundamental* phase current component

$$I_{p}^{b1} = I_{T1}^{1} \quad (5)$$

From (4) and (5), the harmonic entries form the balance phase current *distortion* component

$$I_{p}^{bd} = \sqrt{\left(I_{p}^{b}\right)^2 - \left(I_{p}^{b1}\right)^2} \quad (6)$$

Likewise, the *unbalance* phase current component is defined as

$$I_{p}^{u} = \sqrt{\sum_{n=0}^{\infty}\left[\left(I_{T2}^{3n+1}\right)^2 + \left(I_{T3}^{3n+1}\right)^2 + \left(I_{T1}^{3n+2}\right)^2 + \left(I_{T3}^{3n+2}\right)^2 + \left(I_{T1}^{3n+3}\right)^2 + \left(I_{T2}^{3n+3}\right)^2\right]} \quad (7)$$

and corresponds to the unbalance *fundamental* phase current component

$$I_{p}^{u1} = \sqrt{\left(I_{T2}^{1}\right)^2 + \left(I_{T3}^{1}\right)^2} \quad (7)$$

as well as to the unbalance phase current *distortion* component

$$I_{p}^{ud} = \sqrt{\left(I_{p}^{u}\right)^2 - \left(I_{p}^{u1}\right)^2} \quad (8)$$

Finally, from the above definitions the phase current *distortion* component is expressed in the following forms:

$$I_{p}^{d} = \sqrt{\sum_{h=2}^{\infty}\left[\left(I_{T1}^{h}\right)^2 + \left(I_{T2}^{h}\right)^2 + \left(I_{T3}^{h}\right)^2\right]} = \sqrt{\left(I_{p}^{bd}\right)^2 + \left(I_{p}^{ud}\right)^2} \quad (9)$$

The definitions of the current components have been associated in [10] to the formulation of a set of specific indicators, such as the phase current *balanced distortion* factor

$$\psi_{pI}^{bd} = I_{p}^{bd}\big/I_{p}^{b1} , \quad (10)$$

the phase current *unbalanced distortion* factor

$$\psi_{pI}^{ud} = I_{p}^{ud}\big/I_{p}^{b1} , \quad (11)$$

the phase current *unbalanced distortion* factor at *fundamental* frequency

$$\psi_{pI}^{u1} = I_{p}^{u1}\big/I_{p}^{b1} , \quad (12)$$

and the phase current *overall unbalance* factor

$$\psi_{pI}^{u} = I_{p}^{u}\big/I_{p}^{b1} . \quad (13)$$

Analogous definitions are set up for the system voltages. Furthermore, in [10] the symmetrical component-based definitions are provided also for the neutral current. Correspondingly, the expressions of the equivalent variables (current, voltage and power) representing the entire system in generic conditions of unbalanced and waveform distortion [14,16,17] are deducted, extending the results shown in [18]. The expressions of the equivalent variables consistent with the symmetrical component-based framework are recalled here in the case without neutral current, in the version highlighting the distortion components. The equivalent current and equivalent phase voltage are, respectively,

$$I_{e} = \sqrt{\left(I_{p}^{b1}\right)^2 + \left(I_{p}^{u1}\right)^2 + \left(I_{p}^{d}\right)^2} \quad (14)$$

$$E_{e} = \sqrt{\left(E_{p}^{b1}\right)^2 + \left(E_{p}^{u1}\right)^2 + \left(E_{p}^{d}\right)^2} \quad (15)$$

The equivalent apparent power is expressed in function of its balance, unbalance and distortion terms, as

$$S_{e} = \sqrt{\left(S_{e}^{b}\right)^2 + \left(S_{e}^{u}\right)^2 + \left(S_{e}^{d}\right)^2} \quad (16)$$

where the individual terms are formulated as

$$S_{e}^{b} = 3E_{p}^{b1}I_{p}^{b1} \quad (17)$$

$$S_{e}^{u} = 3\sqrt{\left(E_{p}^{b1}\right)^2\left(I_{p}^{u1}\right)^2 + \left(E_{p}^{u1}\right)^2\left(\left(I_{p}^{b1}\right)^2 + \left(I_{p}^{u1}\right)^2\right)} \quad (18)$$

$$S_{e}^{d} = 3\sqrt{\left(\left(E_{p}^{b1}\right)^2 + \left(E_{p}^{u1}\right)^2\right)\left(I_{p}^{d}\right)^2 + \left(E_{p}^{d}\right)^2\left(I_{p}^{d}\right)^2 + \left(E_{p}^{d}\right)^2\left(\left(I_{p}^{b1}\right)^2 + \left(I_{p}^{u1}\right)^2\right)} \quad (19)$$

III. COMPENSATION OF AN UNBALANCED RESISTIVE SYSTEM

A. Test circuit scheme and compensation principles

The test circuit used in this paper is composed of a resistive load connected to the node terminals *a′* and *c′* of the

three-phase system shown in Fig. 1. These terminals are connected to the supply point through a line represented through its series impedance $\overline{Z}_m = R_m + jX_m$. In the example shown in this paper, we assume $X_m = 0$ for the sake of simplicity in the interpretation of the results. The circuit parameters are $R = 10\ \Omega$ and $R_m = 0.1\ \Omega$. According to the classical theory taking into account non-distorted voltage supply, this system can be compensated by using two reactive components connected as in Fig. 1. The values to be set up for achieving full compensation (i.e., balanced complex currents in the three phases) are $X_C = X_L = \sqrt{3}\,R = 17.3\ \Omega$.
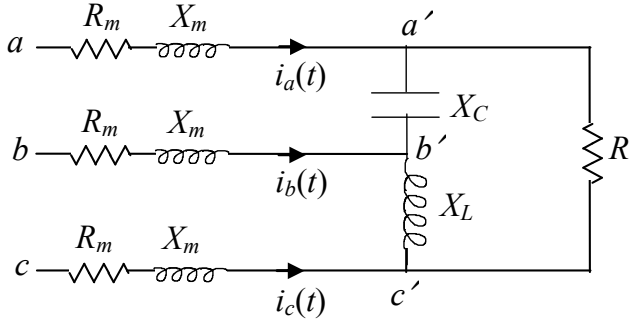

Fig. 1. Unbalanced resistive system with Steinmetz compensation circuit.

B. Results for uncompensated cases

The analysis described in this section is made by using example cases of distorted voltage supply with two superposed three-phase voltage components, one at fundamental frequency (RMS value $E = 400/\sqrt{3}$ V), the other at the 5$^{\text{th}}$ harmonic order (RMS value $E/5$), with the same initial phase angle.

For the initial *uncompensated* resistive system (without the components X_L and X_C), the results of the calculations with distorted voltage supply are shown in Table I for what concerns the RMS currents and voltages. The current unbalance leads to a unity value of the classical unbalance factor. The losses on the three phases (one of which is open) are also reported, as well as the total active power absorbed by the load and generated at the supply terminals. The components and indicators calculated in the proposed framework are indicated in Table II for what concerns the currents, and in Table III for the voltages at the supply terminals. Being the line and load in the system totally resistive, the currents contain the same type of distortion of the supply voltages. As such, the *THD* for voltages and currents is numerically the same. In this case, in the transformed framework, the TPU_I indicator is numerically equal to the current unbalance factor ζ_I^u, and the TPD_I indicator is equal to the THD_I. Table IV reports the equivalent apparent power quantities, as well as the total non-active power $N_e = \sqrt{S_e^2 - P_R^2}$ at the load terminals. From the values reported, the system is mainly unbalanced, while the distortion components are relatively low. This initial situation is taken into account in order to show the properties of the Steinmetz circuitry, with the aim of reaching balanced conditions for the phase currents.

TABLE I
RMS LINE CURRENTS AND VOLTAGES AT THE LOAD TERMINALS FOR THE INITIAL RESISTIVE CIRCUIT WITH DISTORTED VOLTAGE SUPPLY

I_a [A]	39.992	E'_a [V]	232.06	ΔP_a [W]	160
I_b [A]	0	E'_b [V]	235.51	ΔP_b [W]	0
I_c [A]	39.992	E'_c [V]	232.06	ΔP_c [W]	160
THD_{I_a}	0.20	$THD_{E'_a}$	0.20	ΔP_{tot} [W]	320
THD_{I_b}	0	$THD_{E'_b}$	0.20	P_R [W]	15994
THD_{I_c}	0.20	$THD_{E'_c}$	0.20	P_{tot} [W]	16314
ζ_I^u	1.000	$\zeta_{E'}^u$	0.010	-	-

TABLE II
UNBALANCE AND HARMONIC DISTORTION COMPONENTS AND INDICATORS OF THE CURRENTS FOR THE INITIAL RESISTIVE CIRCUIT

I_{T1}^{RMS} [A]	23.090	I_p^u [A]	23.090	ψ_{pI}^{bd}	0.200
I_{T2}^{RMS} [A]	23.090	I_p^{u1} [A]	22.641	ψ_{pI}^{ud}	0.200
I_{T3}^{RMS} [A]	0	I_p^{ud} [A]	4.528	ψ_{pI}^{u1}	1.000
I_p^b [A]	23.090	I_p^d [A]	6.404	ψ_{pI}^u	1.020
I_p^{b1} [A]	22.641	I_e [A]	32.654	TPD_I	0.200
I_p^{bd} [A]	4.528	-	-	TPU_I	1.000

TABLE III
UNBALANCE AND HARMONIC DISTORTION COMPONENTS AND INDICATORS OF THE SUPPLY SIDE VOLTAGES FOR THE INITIAL RESISTIVE CIRCUIT

$E_{T1}^{\prime RMS}$ [V]	233.20	$E_p^{\prime u}$ [V]	45.79	$\psi_{pE'}^{bd}$	0.002
$E_{T2}^{\prime RMS}$ [V]	2.31	$E_p^{\prime u1}$ [V]	2.26	$\psi_{pE'}^{ud}$	0.200
$E_{T3}^{\prime RMS}$ [V]	0	$E_p^{\prime ud}$ [V]	45.74	$\psi_{pE'}^{u1}$	0.010
$E_p^{\prime b}$ [V]	228.68	$E_p^{\prime d}$ [V]	45.74	$\psi_{pE'}^u$	0.200
$E_p^{\prime b1}$ [V]	228.68	E_e' [V]	233.22	$TPD_{E'}$	0.200
$E_p^{\prime bd}$ [V]	0.453	-	-	$TPU_{E'}$	0.200

TABLE IV
EQUIVALENT APPARENT POWER COMPONENTS AND TOTAL NON-ACTIVE POWER FOR THE INITIAL RESISTIVE CIRCUIT

S_e [VA]	22846	S_e^u [VA]	15534	N_e [VA]	16314
S_e^b [VA]	15532	S_e^d [VA]	6275	-	-

C. Results for compensated cases

For the *compensated* system with $X_C = X_L = \sqrt{3}\,R$, the results of the RMS currents and voltage calculations with the same distorted voltage supply considered in the previous section are shown in Table V. In the absence of voltage supply distortion, perfect compensation would be obtained. However, the presence of a distorted supply voltage waveform leads to imperfect phase current balancing, and the nature of the load and of the added Steinmetz circuitry determines relatively different values of THD_I at each phase, while the differences among the THD_E values are clearly much lower. The current unbalance factor ζ_I^u is reduced to zero. Apparently, another effect of the Steinmetz compensation is a reduction of the line losses.

Table VI shows the current components and indicators. The current unbalance factor ζ_I^u corresponds to the indicator ψ_{pI}^{u1}, referred to the fundamental harmonic. In this case, it can be noticed that $\psi_{pI}^{u1} = 0$, but the TPU_I indicator representing the phase unbalance with distorted waveforms has a non-null value. Indeed, in the framework adopted the TPU_I indicator is able to incorporate the reasons why perfect compensation has not been obtained by using the classical set-up for the Steinmetz circuitry. Since $I_p^u = I_p^{ud}$, the effect of unbalance is totally due to the current distortion. Perfect compensation of the phase current unbalance would correspond to $TPU_I = 0$.

In order to investigate the characteristics of the system unbalance, Fig. 2 shows a comparison between the classical unbalance indicator ζ_I^u at fundamental frequency, and the TPU_I indicator, considering as parameters the multipliers m_L and m_C applied to the reactances $X_C = X_L = \sqrt{3}\,R$, in such a way to insert in the circuit the inductive reactance $m_L X_L$ and the capacitive reactance $m_C X_C$, applying the same distorted supply voltage adopted above. The results show that in terms of the classical unbalance indicator the solution with $m_L = m_C = 1$ provides a null value, whereas the unbalance values change by varying the reactance values. However, this evolution does not reflect the true behavior of the system unbalance, since the components at harmonic frequencies are neglected. Looking at the TPU_I indicator, it can be seen that this unbalance indicator does not approach zero, and remains rather far from indicating perfect circuit compensation even by changing the values of the inductive and capacitive reactance of the compensation circuit. For the sake of comparison, Fig. 3 shows that in case of sinusoidal voltage supply (i.e., removing the 5th harmonic from the supply voltage) the TPU_I indicator becomes coincident to the classical unbalance factor. In any case, this evolution cannot be generalized, since it depends on the parameters of the harmonic distortion (amplitude and phase of the individual harmonics).

Table VII shows the components and indicators referred to the load terminal voltages. Again, the classical unbalance factor, equal to the indicator $\psi_{pE'}^{u1}$, is null, but the non-null $TPU_{E'}$ indicates the presence of residual voltage unbalance. Finally, Table VIII reports the power quantities. The null value of the unbalance apparent power S_e^u is determined by substituting the null components $E_p'^{u1} = 0$ (the specific voltage at the load terminals) and $I_p^{u1} = 0$ in the general expression (18).
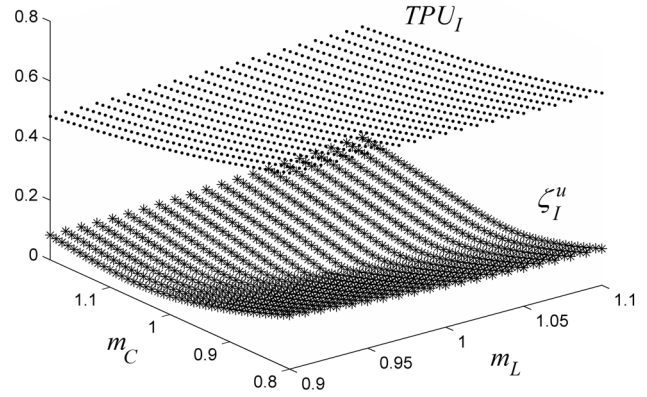

Fig. 2. Unbalance indicators for different multipliers of the Steinmetz compensating reactance values (distorted supply voltage).
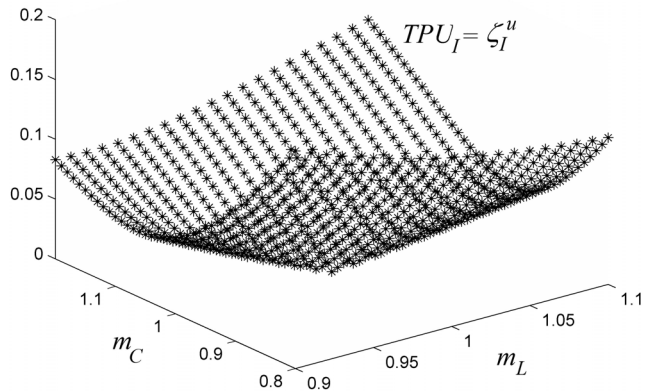

Fig. 3. Unbalance indicators for different multipliers of the Steinmetz compensating reactance values (non-distorted supply voltage).

TABLE V
RMS LINE CURRENTS AND VOLTAGES AT THE LOAD TERMINALS FOR THE COMPENSATED CIRCUIT

I_a [A]	28.285	E_a' [V]	233.35	ΔP_a [W]	80
I_b [A]	32.086	E_b' [V]	233.03	ΔP_b [W]	103
I_c [A]	23.995	E_c' [V]	233.14	ΔP_c [W]	58
THD_{I_a}	0.728	$THD_{E_a'}$	0.204	ΔP_{tot} [W]	241
THD_{I_b}	0.984	$THD_{E_b'}$	0.197	P_R [W]	15557
THD_{I_c}	0.318	$THD_{E_c'}$	0.199	P_{tot} [W]	15798
ζ_I^u	0	$\zeta_{E'}^u$	0	-	-

TABLE VI
UNBALANCE AND HARMONIC DISTORTION COMPONENTS AND INDICATORS OF THE CURRENTS FOR THE INITIAL RESISTIVE CIRCUIT

I_{T1}^{RMS} [A]	26.650	I_p^u [A]	13.689	ψ_{pI}^{bd}	0.418
I_{T2}^{RMS} [A]	9.569	I_p^{u1} [A]	0	ψ_{pI}^{ud}	0.599
I_{T3}^{RMS} [A]	0	I_p^{ud} [A]	13.689	ψ_{pI}^{u1}	0
I_p^b [A]	24.787	I_p^d [A]	16.702	ψ_{pI}^u	0.599
I_p^{b1} [A]	22.865	I_e [A]	28.316	TPD_I	0.730
I_p^{bd} [A]	9.569	-	-	TPU_I	0.552

TABLE VII
UNBALANCE AND HARMONIC DISTORTION COMPONENTS AND INDICATORS OF THE LOAD TERMINAL VOLTAGES FOR COMPENSATED CIRCUIT

$E_{T1}'^{RMS}$ [V]	233.17	$E_p'^u$ [V]	45.68	$\psi_{pE'}^{bd}$	0.004
$E_{T2}'^{RMS}$ [V]	0.96	$E_p'^{u1}$ [V]	0	$\psi_{pE'}^{ud}$	0.200
$E_{T3}'^{RMS}$ [V]	0	$E_p'^{ud}$ [V]	45.68	$\psi_{pE'}^{u1}$	0
$E_p'^b$ [V]	228.66	$E_p'^d$ [V]	45.69	$\psi_{pE'}^{u}$	0.200
$E_p'^{b1}$ [V]	228.65	E_e' [V]	233.17	$TPD_{E'}$	0.200
$E_p'^{bd}$ [V]	0.957	-	-	$TPU_{E'}$	0.200

TABLE VIII
EQUIVALENT APPARENT POWER COMPONENTS AND TOTAL NON-ACTIVE POWER FOR THE COMPENSATED CIRCUIT

S_e [VA]	19807	S_e^u [VA]	0	N_e [VA]	12260
S_e^b [VA]	15685	S_e^d [VA]	12096	-	-

D. Variation of the supply voltage distortion parameters

Other analyses have been carried out in order to study the effects of the variation of the amplitude and phase angle of the supply voltages on the various indicators. For instance, the variation of the fifth harmonic has been considered, expressed by the 5th harmonic voltage amplitude multiplier with respect to the fundamental supply phase RMS voltage E. Fig. 4 shows the unbalance representation through the TPU_I indicator. The classical unbalance indicator is null in all the cases shown, and is clearly unsuitable to represent the compensation effect in the presence of waveform distortion.

Fig. 5 shows the variation of the transformed phase current components. Since the system is not perfectly balanced, the effect of the 5th harmonic waveform distortion is not totally rooted into the unbalance component, but in part goes to increase the balance current component. Fig. 6 illustrates how the TPD_I indicator can provide a single information (in this case very close but anyway not coincident with the THD of the current at phase 1) that synthesizes the three THD values of the currents at the different phases.
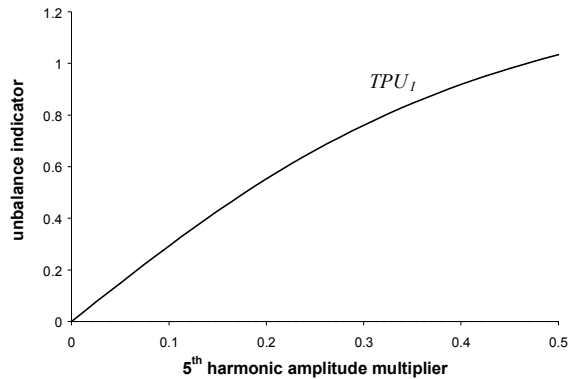

Fig. 4. TPU_I indicator for the compensated circuit with different values of the 5th harmonic amplitude multiplier.

In more detail, the variation of the TPU_I indicator has been addressed for different values of the 5th harmonic multiplier (from 0 to 0.5) and for different phase angles of the 5th harmonic (from 0 to 1.2 radians, with the upper limit chosen to be close to $2\pi/5$ radians). Fig. 7 shows the resulting values of

the TPU_I indicator. In this case, for the same 5th harmonic multiplier, the characteristics of the circuit lead to reaching the maximum unbalance for a certain 5th harmonic phase angle.
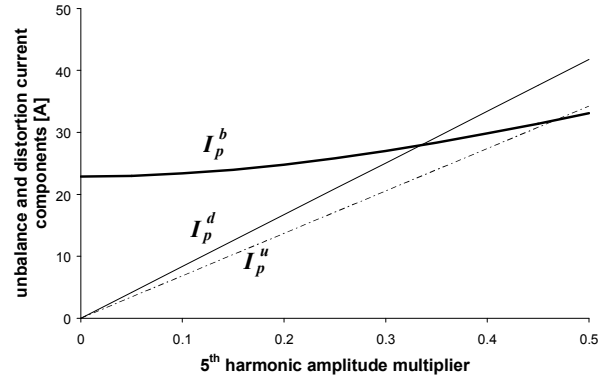

Fig. 5. Balance, unbalance and distortion current components for the compensated circuit with different values of the 5th harmonic amplitude multiplier.
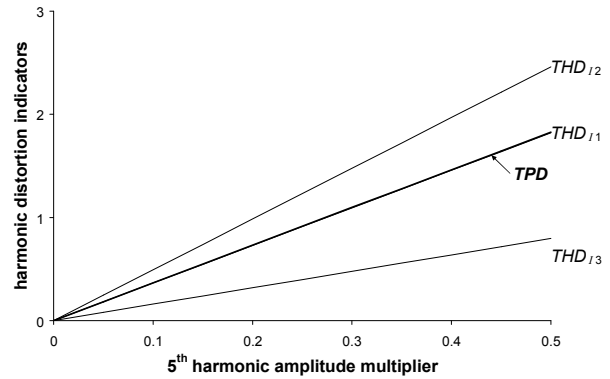

Fig. 6. Harmonic distortion indicators for the compensated circuit with different values of the 5th harmonic amplitude multiplier.

Concerning the equivalent power components, by varying the 5th harmonic multiplier and the 5th harmonic phase angle in the ranges shown below, in all cases the S_e^b component is the same, equal to 15685 VA, and the S_e^u component is always null. For the S_e^d component (Fig. 8), its maximum values are reached around the 5th harmonic phase angle of $\pi/5$ radians.

IV. CONCLUSIONS

This paper has shown how the properties of the Steinmetz compensation circuit in an illustrative case of single-phase load balancing depend on the waveform distortion. A tutorial example with the 5th harmonic as distorting component has been constructed, varying its amplitude and phase angle.

The results shown confirm the effectiveness of the indicators defined in the symmetrical component-based framework to explain the properties of the Steinmetz circuitry operating under waveform distortion. In particular, the TPU indicator provides the correct information also when the classical unbalance indicator is unable to detect lack of circuit balancing because of the effects of waveform distortion. Results for more general cases of application of the concepts proposed here will be reported in the future.
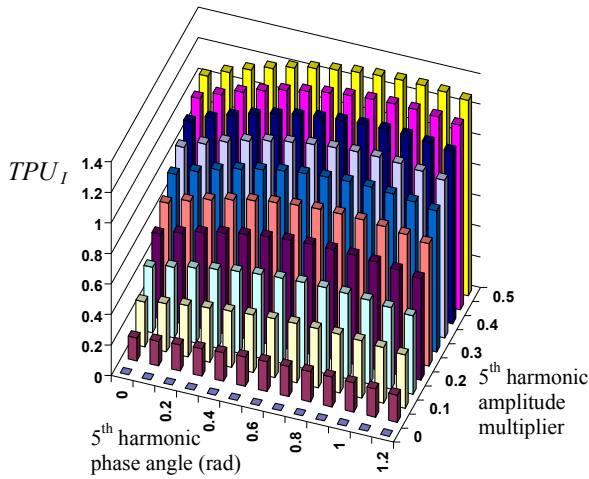
Fig. 7. TPU_I indicator for the compensated circuit with different values of the 5th harmonic phase angle and amplitude multiplier.
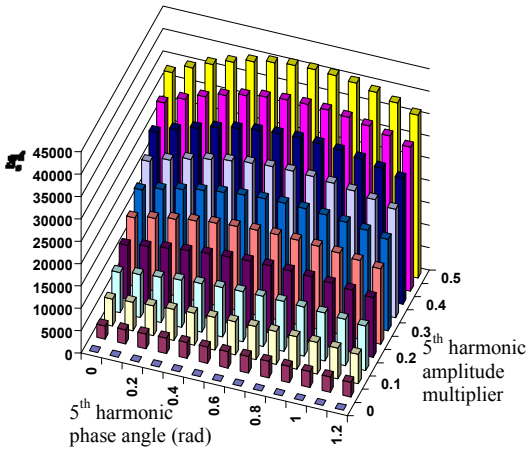

Fig. 8. S_e^d component in the compensated circuit with different values of the 5th harmonic phase angle and amplitude multiplier.

V. REFERENCES

[1] C.P. Steinmetz, *Lectures on Electrical Engineering*, Dover, New York, 1897.

[2] L. Gyugyi, R. A. Otto and T. H. Putman, Principles and applications of static thyristor-controlled shunt compensators, *lEEE Trans. Power Apparatus and System*s, **PAS-97** (5), 1978, 1935-1945.

[3] M. Chindriş, A. Cziker and S. Ştefanescu, Fuzzy Logic Controller for Steinmetz Symmetrizing Circuitry with Variable Reactor, *Proc. IEEE Porto Power Tech Conference*, Porto, Portugal, September 10 -13, 2001.

[4] G. Todeschini, A.E. Emanuel, A. Ferrero and A.P.Morando, A Poynting Vector Approach to the Study of the Steinmetz Compensator, *IEEE Trans. on Power Delivery* **22** (3), July 2007, 1830-1833.

[5] M. Chindriş, A. Cziker and S. Ştefanescu, Symmetrizing Steinmetz circuitry behavior in harmonic polluted networks, *Proc. ClRED2001*, Amsterdam, The Netherlands, June 18-21, 2001, IEE Conference Publication No. 482, paper 2.42.

[6] O. Jordi, L. Sainz, and M. Chindris, Steinmetz system design under unbalanced conditions, *ETEP* **12** (4), July/August 2002, 283–290.

[7] L. Sainz, J. Pedra and M. Caro, Steinmetz Circuit Influence on the Electric System Harmonic Response, *IEEE Trans. on Power Delivery* **20** (2), April 2005, 1143-1150.

[8] M. Caro, L. Sainz, and J. Pedra, Study of the power system harmonic response in the presence of the Steinmetz circuit, *Electric Power Systems Research* **76** (12), August 2006, 1055–1063.

[9] L. Sainz, J. Pedra and M. Caro, Influence of the Steinmetz Circuit Capacitor Failure on the Electric System Harmonic Response, *IEEE Trans. on Power Delivery* **22** (2), April 2007, 960-967.

[10] G. Chicco, P. Postolache and C. Toader, Analysis of three-phase systems with neutral under distorted and unbalanced conditions in the symmetrical component-based framework, *IEEE Trans. on Power Delivery* **22** (1), January 2007, 674-683.

[11] F. Batrinu, G. Chicco, A.O. Ciortea, R. Porumb, P. Postolache, F. Spertino and C. Toader, Experimental Evaluation of Unbalance and Distortion Indicators in Three-Phase Systems with Neutral, *Proc. IEEE PowerTech 2007*, Lausanne, Switzerland, 1-5 July 2007, paper 527.

[12] A.M. Stanković, S.R. Sanders and T. Aydin, Dynamic Phasors in Modeling and Analysis of Unbalanced Polyphase AC Machines, *IEEE Trans. Energy Conv.* **17** (1), March 2002, 107-113.

[13] G.C. Paap, Symmetrical Components in the Time Domain and Their Application to Power Network Calculations, *IEEE Trans. Pow. Syst.* **15** (2), May 2000, 522-528.

[14] M. Depenbrock, The FBD-method, a generally applicable tool for analyzing power relations, *IEEE Trans. Pow. Syst.* **8** (2), May 1993, 381-387.

[15] M. Depenbrock and V. Staudt, Discussion of "Practical definitions for powers in systems with nonsinusoidal waveforms and unbalanced loads: a discussion", *IEEE Trans. Pow. Deliv.* **11** (2), April 1996, 89-90.

[16] A.E. Emanuel, On the assessment of Harmonic Pollution, *IEEE Trans. Pow. Deliv.* **10** (3), July 1995, 1693-1698.

[17] IEEE Working Group on nonsinusoidal situations, Practical definitions for powers in systems with nonsinusoidal waveforms and unbalanced loads: a discussion, *IEEE Trans. Pow. Deliv.* **11** (1), Jan. 1996, 79-101.

[18] T. Zheng, E.B. Makram and A.A. Girgis, Evaluating power system unbalance in the presence of harmonic distortion, *IEEE Trans. Pow. Deliv.* **18** (2), April 2003, 393–397.

[19] CENELEC (European Committee for Electrotechnical Standardisation), *Voltage characteristics of electricity supplied by public distribution systems*, European Norm EN 50160, 1994.

[20] IEEE Trial-Use Standard: Definition for the Measurement of Electric Power Quantities Under Sinusoidal, Nonsinusoidal, Balanced, or Unbalanced Conditions, *IEEE Std. 1459*, 2000.

VI. BIOGRAPHIES

Gianfranco Chicco (M'98, SM'08) received the Ph.D. degree in Electrotechnical Engineering from Politecnico di Torino (PdT), Torino, Italy, in 1992. Currently, he is an Associate Professor of Electric Distribution Systems at PdT. His research interests include power system and distribution system analysis, competitive electricity markets, energy efficiency, load management, artificial intelligence applications, and power quality. He is a member of AEIT.

Mircea Chindriş (M'06) received the M.S. degree and the Ph.D. degree in Electrical Engineering from the Technical University of Cluj-Napoca, Romania. In 1974 he joined the same University where he is presently a Full Professor in the Electrical Power Systems Department. His technical interests are in power systems harmonics and power quality, energy management and electrical technologies.

Andrei Cziker received the M.S. degree in Physics from the "Babes-Bolyai" University of Cluj-Napoca, Romania, in 1995, and the M.S. degree in Electrical Engineering from Technical University of Cluj-Napoca in 1998. He is presently an Associate Professor at the Technical University of Cluj-Napoca. His technical interests are in energy management and power quality.

Petru Postolache (M'01) received the M.Sc. degree in Electrical Engineering and the Ph.D. degree from the University Politechnica Bucharest (UPB), Bucharest, Romania. Currently, he is a Full Professor with the Electric Power Engineering Department at the UPB. His main research interests include electrical energy efficiency, power distribution, electrical disturbances, and power quality analysis. He is Member of the National Romanian Committee of CIRED and Chairman of its SC4.

Cornel Toader (M'01) received the M.Sc. and Ph.D. degrees from the University Politehnica Bucharest (UPB), Romania, in 1968 and 1988, respectively. Currently, he is a Full Professor of Electric Energy Utilization at the UPB and the Head of the Electric Energy Utilization Group of the Electric Power Engineering Department. His research interests include power quality analysis, network modeling, and electrotechnologies.